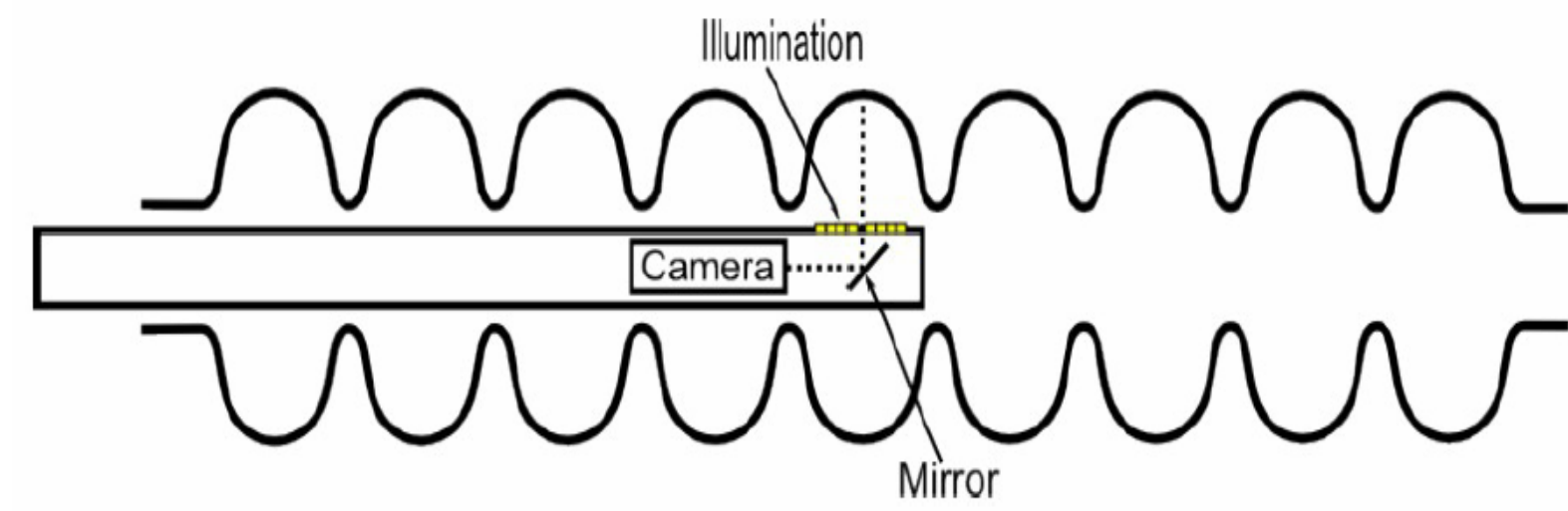


# CHARACTERIZATION OF OPTICAL SURFACE PROPERTIES OF 1.3 GHZ SRF CAVITIES FOR THE EUROPEAN XFEL



Marc Wenskat, Lea Steder – DESY Hamburg

## Optical Inspection and Automated Image Analysis



Sketch of cavity with camera. The camera is viewing the inner surface via a 45 degree mirror. The illumination stripes are placed on the outside of the rod adjacent to the optical path.

### OBACHT

A fully automated robot for optical inspection has been routinely used at DESY since 2012. It is equipped with a high-resolution camera and resolves structures down to 12  $\mu\text{m}$  for properly illuminated surfaces. [1,2]

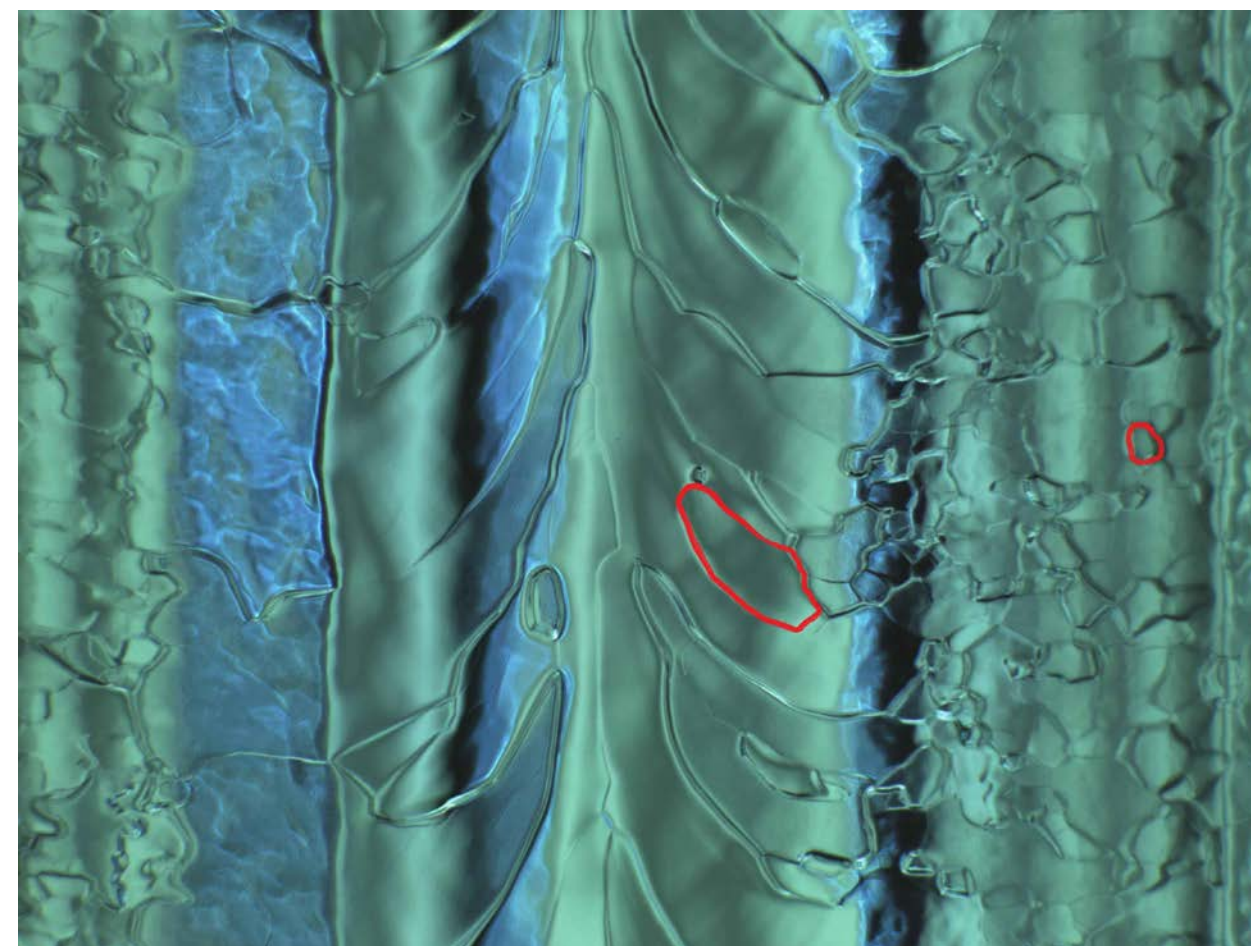
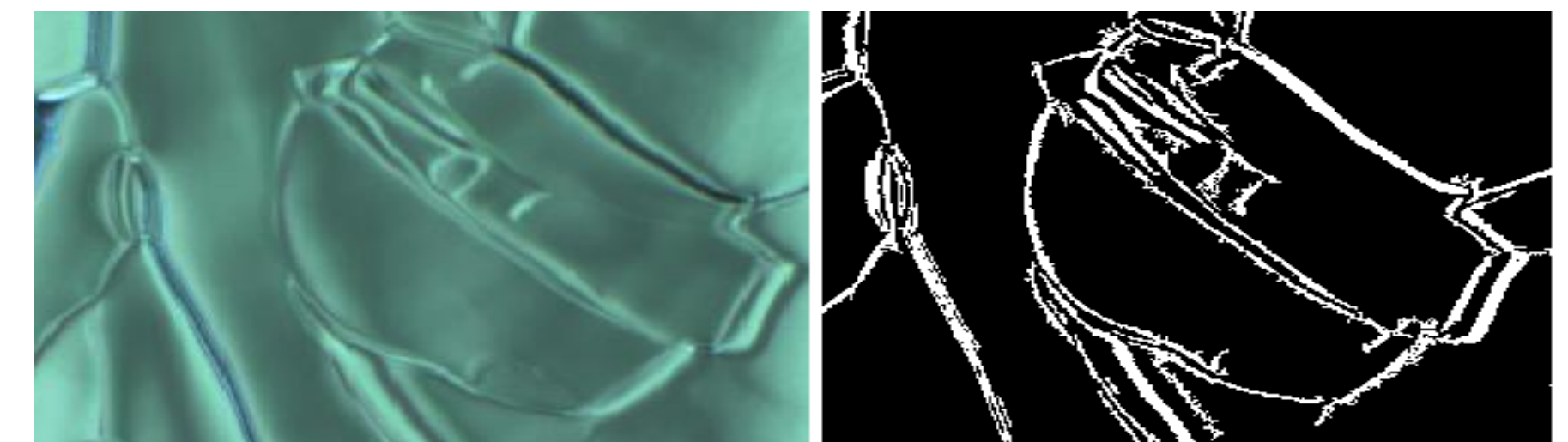


Image of the inner cavity surface with the welding seam in the image center taken with OBACHT. The image dimension is 9 x 12 mm<sup>2</sup>. The red contours are examples of grain boundaries identified with the image processing algorithm.



On the left, a detail of an OBACHT image is shown. The image on the right is the same detail after the image processing algorithm.

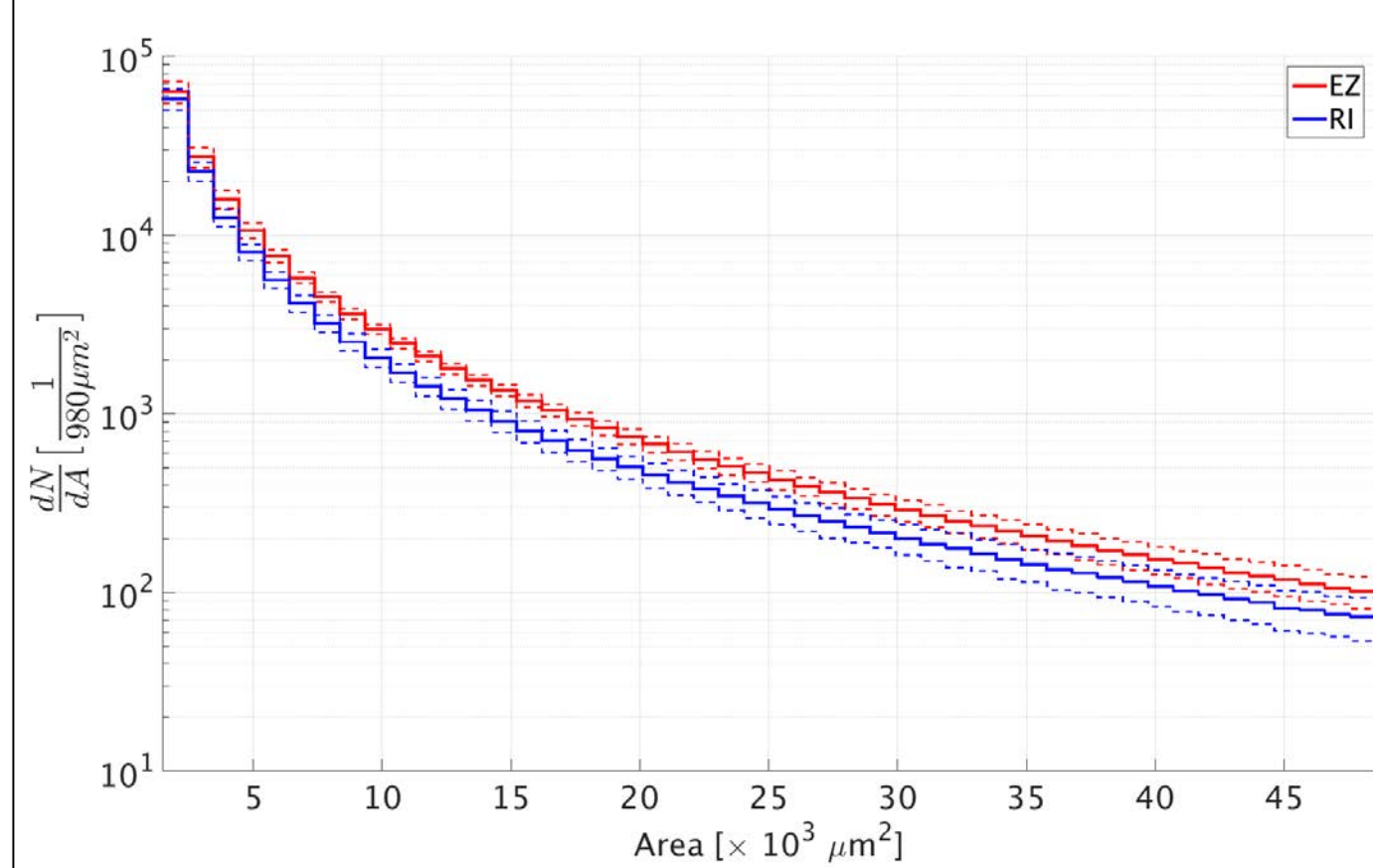
### Image Processing Algorithm

An algorithm has been developed to correct for illumination variations, image noise and to identify grain boundaries regardless of their surrounding. [2]

Output of this algorithm is a binary image which contains all information of the relation of a pixel to its neighbors and thereby individual grain boundaries are identified.

Based on this labeled binary image, properties of the individual boundaries are obtained.

## Surface Characterization



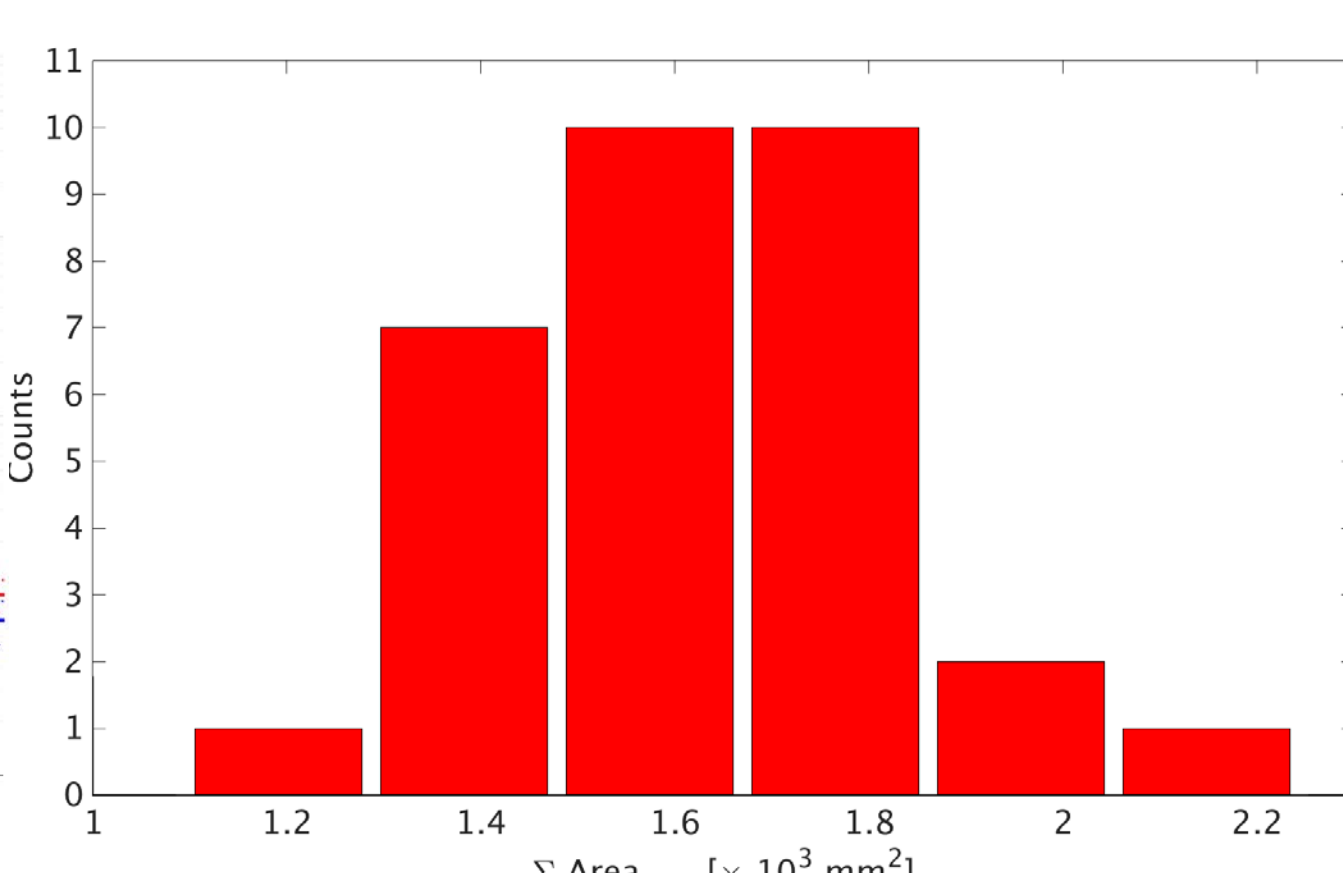
Average grain boundary area distribution of an equator. The blue distribution shows the average of 126 Research Instruments (RI) equators, the red distribution shows the average of 279 Ettore Zanon (EZ) equators. The dotted lines are the 1 $\sigma$  confidence intervals of the average.

### Grain Boundary Area Distribution

The grain boundary area  $A$  is the total amount of pixels a grain boundary consists of in the binary image times the *pixel size*, which is 12.25  $\mu\text{m}$  for OBACHT.

A vendor specific distribution has been observed.

Research Instruments cavities are seen to exhibit fewer objects of large grain boundary area.



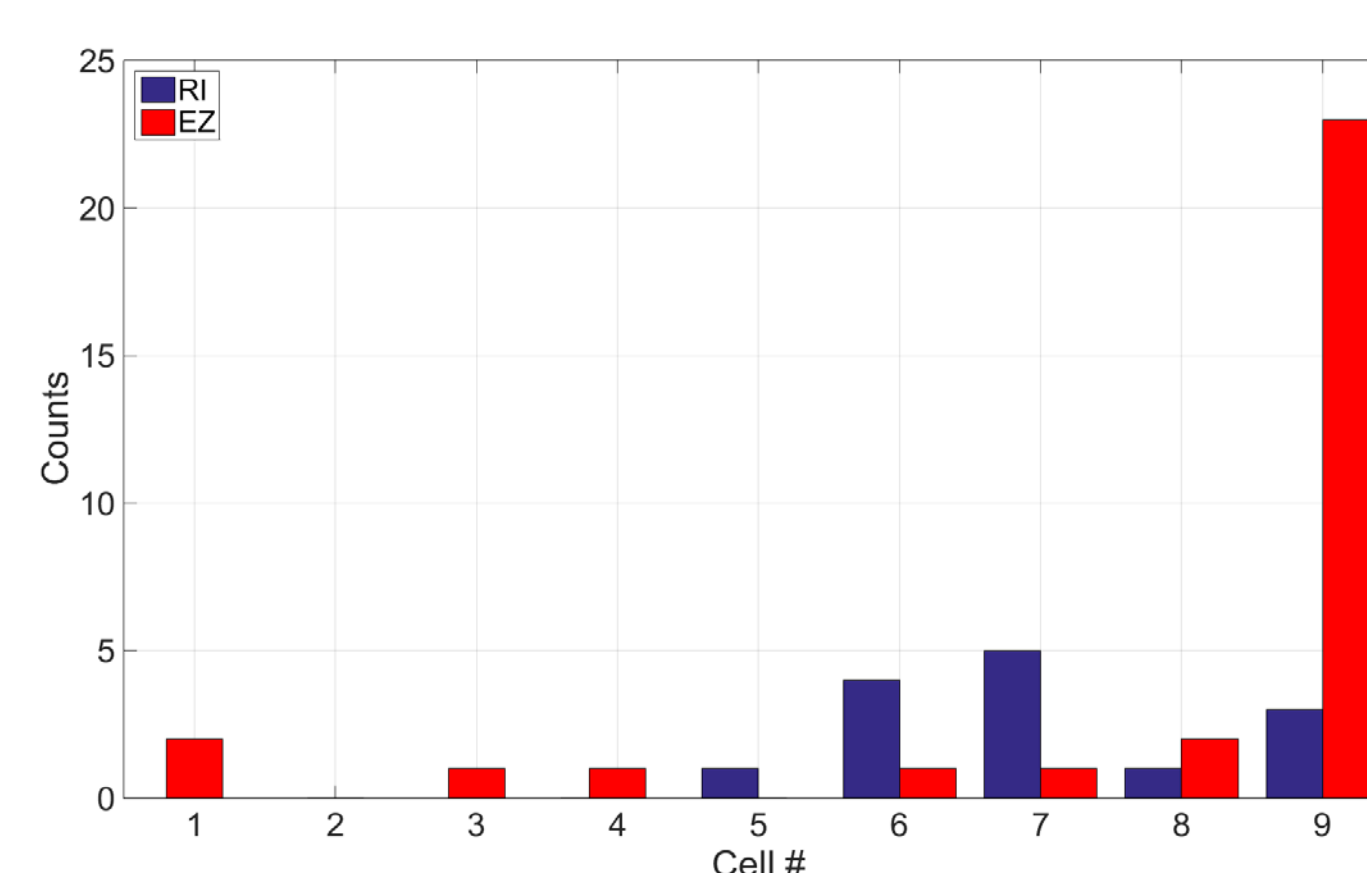
Histogram of the values of the integrated grain boundary area for the optically conspicuous cells from Ettore Zanon.

### Values for Optically Conspicuous Cell

The *integrated grain boundary area*  $\Sigma A$  is the total grain boundary area identified in the equator region.

The cell with the largest integrated grain boundary area of an individual cavity is called the *optically conspicuous cell*.

The integrated grain boundary area averages at about 1600 mm<sup>2</sup>, hence covering about 20% of the weld area, for Ettore Zanon and about 1200 mm<sup>2</sup> for Research Instruments

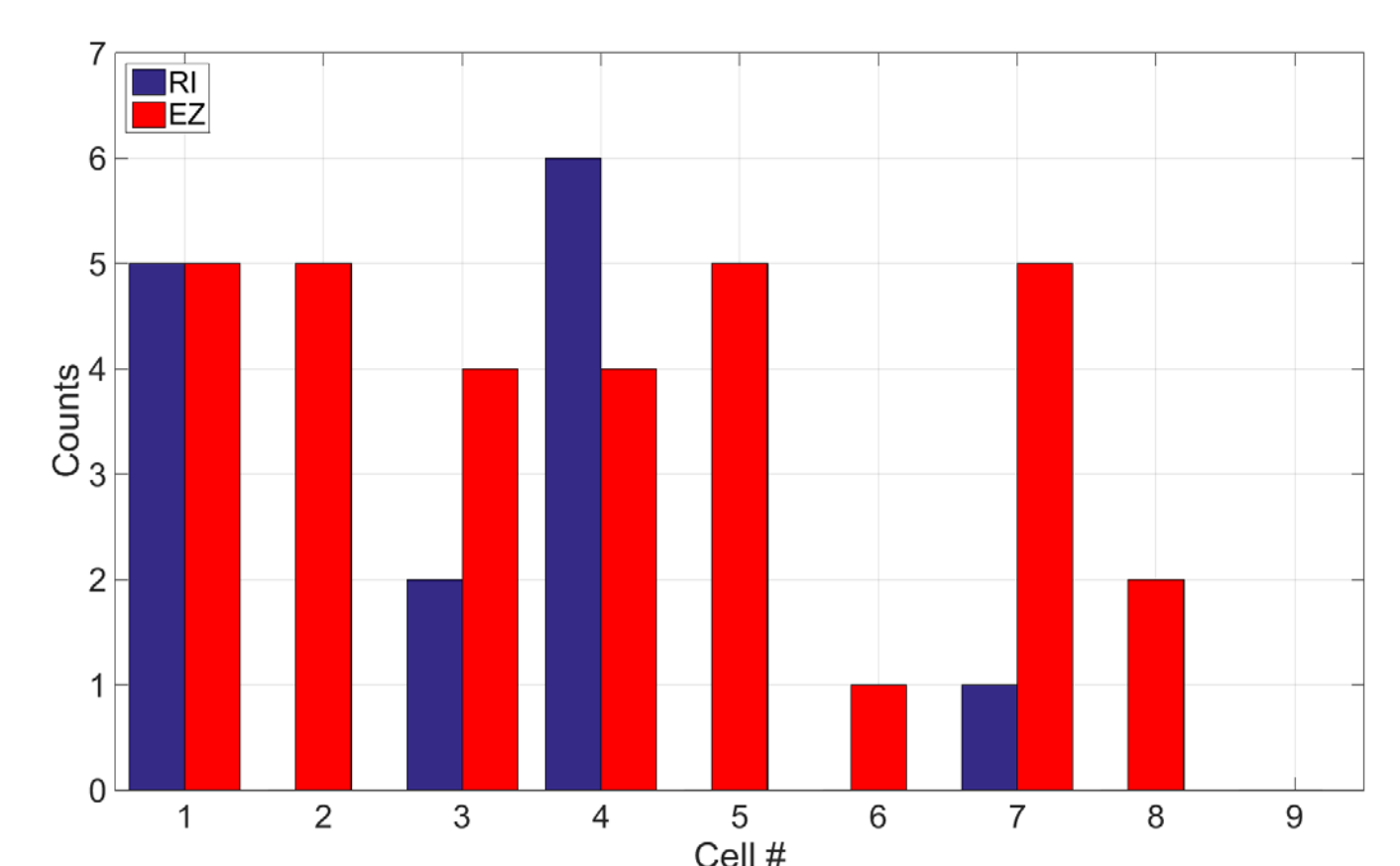


Observed longitudinal distribution of the optically conspicuous cell. The blue distribution is derived from 14 Research Instruments (RI) cavities, the red distribution from 31 Ettore Zanon (EZ) cavities.

### Distribution of Optically Conspicuous Cell

A vendor specific distribution of the optically conspicuous cell has been observed.

An excess in equator 9 for Ettore Zanon is observed. An asymmetry for Research Instruments with a small excess at equators 6 and 7 is observed.



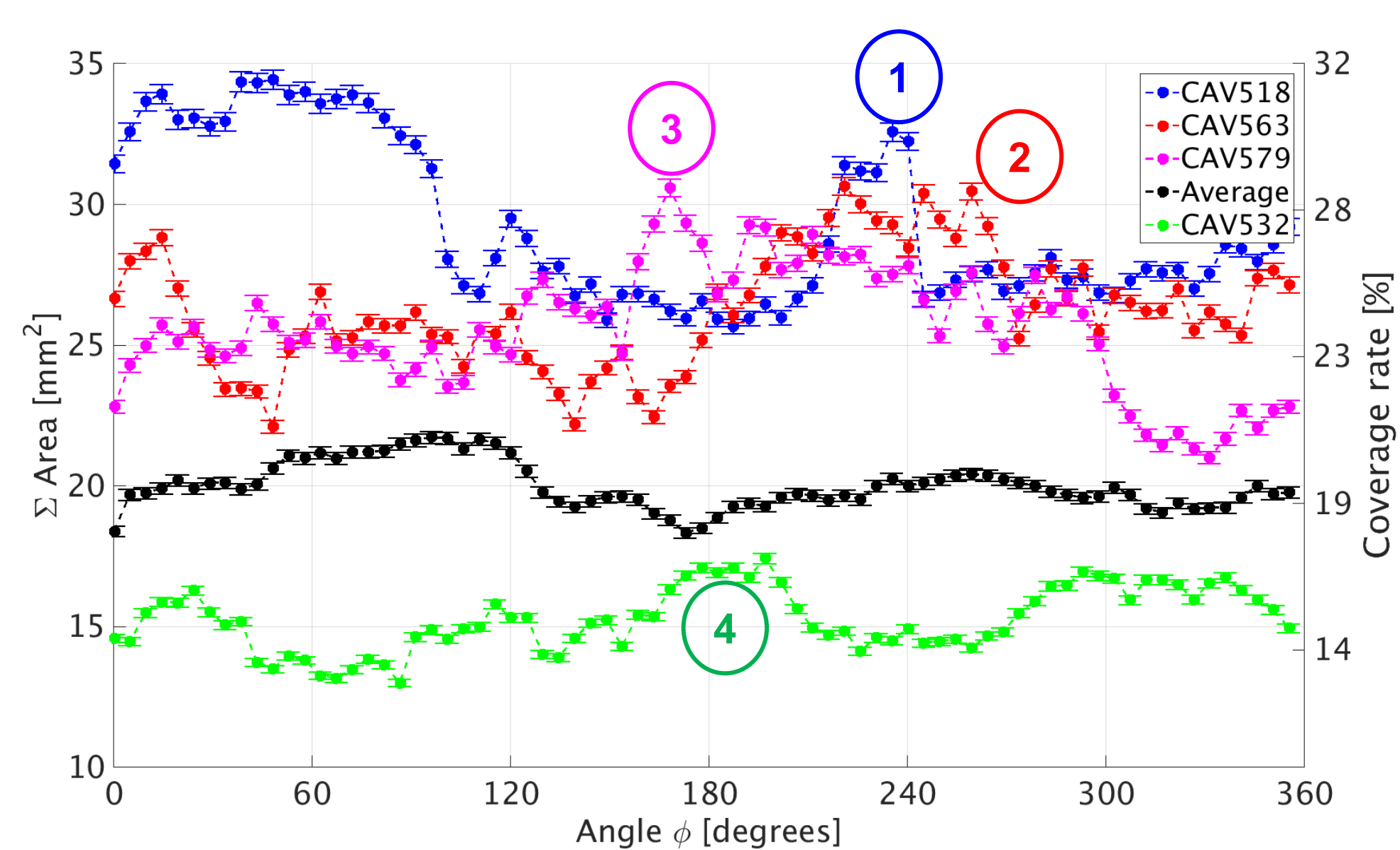
Observed longitudinal distribution of the optically best cell. The blue distribution is derived from 14 Research Instruments (RI) cavities, the red distribution from 31 Ettore Zanon (EZ) cavities.

### Distribution of Optically Best Cell

The cell with the smallest integrated grain boundary area of an individual cavity is called the *optically best cell*.

A priori, a uniform distribution is expected. The observed distribution is in agreement with the expectation, although the  $\chi^2$  for Research Instruments is rather large ( $\chi^2=32$ ,  $df=8$ ).

## Equatorial Weld of Optically Conspicuous Cells



Integrated grain boundary area (per image) against angular position of the image taken for the three cells with the largest values, the average of the whole set and the cell with the smallest value. The numbers indicate the image shown on the right.

### Contributions to Integrated Grain Boundary Area

- ① CAV518 – Repair of equatorial weld / remnants of machining in heat affected zone
- ② CAV563 – Prominent grain boundaries on weld and heat affected zone
- ③ CAV579 – Prominent grain boundaries on weld and heat affected zone
- ④ CAV532 – Smooth and homogenous weld and heat affected zone

Noticeable surface and welding features correspond to peaks in the distributions.

Cavity	$\langle \Sigma A \rangle$ per Image	$E_{\text{acc,max}}$
CAV518	28 mm <sup>2</sup>	22 MV/m
CAV563	26 mm <sup>2</sup>	20 MV/m
CAV579	25 mm <sup>2</sup>	25 MV/m
$\langle \text{EZ} \rangle$	$21 \pm 2$ mm <sup>2</sup>	$28 \pm 7$ MV/m
CAV532	15 mm <sup>2</sup>	35 MV/m

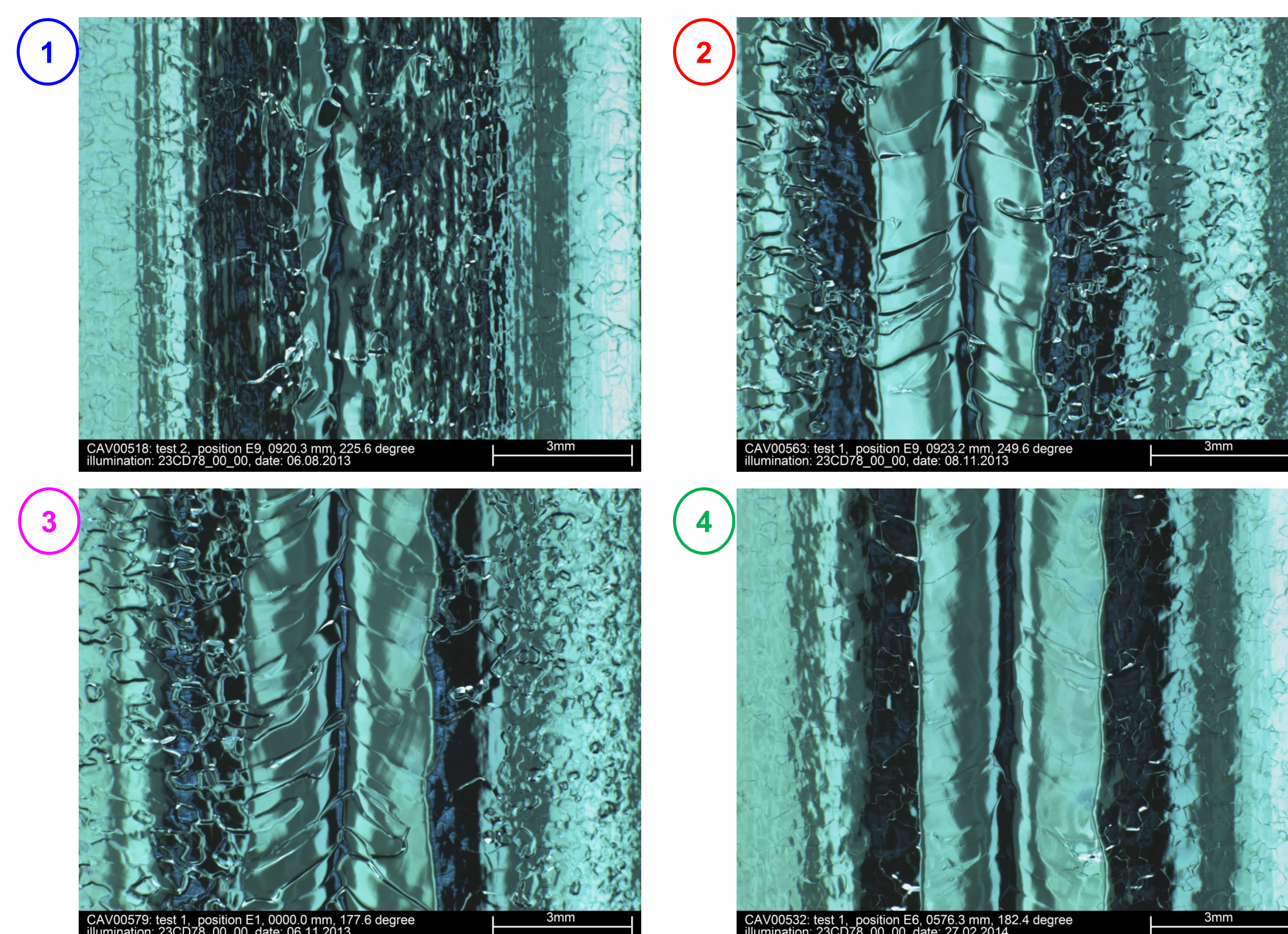
RF results and the integrated grain boundary area per image for the cavities in this data set.

### Comparison of RF Results and Integrated Grain Boundary Area

Motivation for the definition of the integrated grain boundary area was that grain boundaries contribute to losses.

The table compares the observed average integrated grain boundary area and the achieved accelerating field.

Results suggest that higher  $E_{\text{acc,max}}$  can be reached when the integrated grain boundary area is small. [2]



## Summary

- Automated image analysis algorithm developed  
Useful for quality assurance of a large scale production
- First time: optical characterization of inner cavity surface  
Quantitative global quantization describing grain boundary topography
- Influence of optical surface properties on performance studied  
Correlations are observed, although the underlying cause remain unidentified



Unterstützt von / Supported by



Funding from the EU 7<sup>th</sup> Framework Program (FP7/2007-2013 under agreement number 283745 (CRISP) and "Construction of New Infrastructures – Preparatory Phase", ILC-HiGrade, contract number 206711, BMBF project 05H12GU9 and Alexander von Humboldt Foundation

### References

[1] M. Lemke et al., "OBACHT - Optical Bench for Automated Cavity Inspection with High Resolution on Short Time Scales", ILC-HiGrade-Report-2013-001 (2013)

### Acknowledgements

J. Iversen, D. Reschke, W. Singer / MHF-sl - A. Matheisen / MKS3 - A. Navitski, J. Schaffran, Y. Tamashovich / FLA-ILC S. Aderhold / Fermilab

[2] M. Wenskat, "Automated Surface Classification of SRF Cavities for the Investigation of the Influence of Surface Properties onto the Operational Performance", PhD thesis, University of Hamburg, 2015

